

Achievable Roll Stability of Heavy Road Vehicles

David J. M. Sampson*

David Cebon†

Cambridge University Engineering Department

Trumpington St, Cambridge CB2 1PZ, UK

December 19, 2001

Submitted to *Proc. IMechE, Journal of Automobile Engineering*

*Present address: The MathWorks, Matrix House, Cowley Park, Cambridge CB4 0HH, UK

†Corresponding author, e-mail dc@eng.cam.ac.uk

Summary

A general purpose numerical model, suitable for simulating the yaw-roll behaviour of torsionally flexible heavy goods vehicles with an arbitrary arrangement of vehicle units, is presented. A controllability analysis is then performed to examine the fundamental limitations in achievable roll stability of heavy vehicles with active roll control systems. It is established that it is not possible to control simultaneously and independently all axle load transfers and body roll angles. The best achievable control objective for maximising roll stability is shown to be setting the normalised load transfers at all critical axles to be equal, while taking the largest inward suspension roll angle to the maximum allowable angle. The results of a simulation of a tractor semi-trailer vehicle with a full-state feedback active roll control system are presented. It is shown that the roll stability of the vehicle can be increased by 30-40% for steady state and transient manoeuvres and that the handling behaviour improves significantly.

1 Introduction

1.1 Roll-over of heavy vehicles

The roll-over of heavy vehicles is an important road safety problem world-wide. Several studies have reported that a significant proportion of the serious heavy vehicle accidents involve roll-over. For example, in 1996 and 1997, the US National Highway Traffic Safety Administration documented over 15000 roll-over accidents per year involving commercial heavy vehicles [1, 2].

A review of heavy vehicle safety by von Glasner considered that while some roll-over accidents involving articulated vehicles were preventable given a sophisticated warning system and a highly skilled driver, the majority could only be avoided by the intervention of advanced active safety systems [18]. Winkler et al. also noted that it is very difficult for truck drivers to perceive their proximity to roll-over while driving [19, 21].

Winkler et al. surveyed US accident statistics and reported a strongly negative correlation between steady-state roll stability and the average likelihood of roll-over accidents [19, 20, 22]. The study found that an increase in the static roll-over threshold of 0.1 g in the range 0.4-0.7 g caused a 50% reduction in the frequency of roll-over accidents for tractor semi-trailer combinations. For example, the average frequency of roll-over accidents was 0.16 events per million kilometres travelled among vehicles with a static rollover threshold of 0.5 g but 0.07 events per million kilometres among vehicles with a static roll-over threshold of 0.6 g. The study also established a link between steady-state roll stability and the probability of roll-over in an accident. Roll-over accidents accounted for almost 50% of non-jack-knife accidents to tractor semi-trailers with a static roll-over threshold of 0.4 g but less than 15% to tractor semi-trailers with a roll-over threshold of 0.6 g. Interestingly these statistics indicate that drivers do not drive less stable vehicles more cautiously (and conversely, do not drive more stable vehicles less cautiously). This is believed to be because drivers are unable to assess roll-over stability accurately while driving.

It is clear that even a modest increase in roll stability can lead to a significant reduction in the frequency of roll-over accidents.

1.2 Review of previous work

Recently the use of active roll control systems to improve vehicle roll stability and reduce the likelihood of roll-over accidents has been proposed by several authors. Vehicles with conventional passive suspensions tilt out of corners under the influence of lateral acceleration. The centre of sprung mass shifts outboard of the vehicle centreline and this contributes a destabilising moment that reduces roll stability. The aim of a stabilising active roll control system is to lean the vehicle *into* corners such that the centre of sprung mass shifts inboard of the vehicle centreline and contributes a stabilising roll moment.

Dunwoody and Froese used simulations to investigate the potential benefits of using an active roll control system to increase the steady-state roll stability of a tractor semi-trailer [5]. The roll control system hardware was contained entirely within the trailer unit and consisted of a tiltable fifth wheel coupling and hydraulic actuators at the trailer axles. The sole input to the roll controller was a lateral acceleration signal from an accelerometer mounted on the trailer. Controller gains were selected using a simple steady-state roll-plane model. The authors concluded that the system could increase the roll-over threshold by 20-30% for a wide range of trailer loading conditions.

Lin et al. investigated the use of an active roll control system to reduce the total lateral load response of a single unit truck to steering inputs [9, 12]. A linear model with four degrees of freedom (yaw, sideslip, sprung mass roll angle and unsprung mass roll angle) was used. A steering input spectrum was derived by considering the low frequency steering inputs required to follow the road (based on road alignment data) as well as the higher frequency inputs needed to perform frequent lane change manoeuvres. This spectrum was used to design an optimal full-state, linear quadratic controller to regulate load transfer. This control scheme caused the vehicle to lean into

corners. The lateral acceleration level at which wheel lift-off was first experienced was increased by 66% and the RMS load transfers in response to a random steering input were reduced by 34%. A proportional-derivative lateral acceleration feedback controller was also designed using pole placement. Although the reductions in total load transfer were smaller, the lateral acceleration controller was attractive because of its simpler instrumentation requirements.

Lin et al. also investigated the use of active roll control to enhance the roll stability of a tractor semi-trailer [9, 11]. The design of the roll control system was performed using a seven degree of freedom linear model. The controller used lateral acceleration signals from the tractor and trailer to control active anti-roll bars fitted to the tractor and trailer axles. The proportional controller gains were selected for good steady-state roll stability and the derivative gains were chosen to equate the normalised RMS load transfers of the two units. The system reduced steady-state and transient load transfers by up to 30%. Results were confirmed by time domain simulations using a validated nonlinear yaw-roll model [10]. The authors noted that the transfer of roll moment across the fifth wheel coupling allowed the roll control system on the tractor to contribute to the roll stability of the trailer.

1.3 Research needs

Despite this previous work, the nature of fundamental limitations in achievable roll stability for vehicles with active roll control systems is not well understood. An understanding of these limitations is necessary to enable the formulation of achievable control system design objectives that maximise vehicle roll stability. In addition, the effects of the torsional flexibility of vehicle frames and couplings and the lift-off of individual axles on the roll stability of heavy vehicles with active roll control systems must be considered.

2 Vehicle models

2.1 Single unit vehicle model

The roll and handling response of a single unit vehicle to steering inputs was investigated using a linear model that built on models formulated by Segel [15] and Lin [9]. Pitching and bouncing motions have only a small effect on the roll and handling behaviour of the vehicle and so were neglected. The effects of aerodynamic inputs (wind disturbances) and road inputs (cross-gradients, dips and bumps) were also neglected.

2.1.1 Rigid frame model

The single unit vehicle was modelled using three rigid bodies – one to represent the sprung mass, and one each for the front and rear axle group – as shown in figure 1. For vehicles with multiple axles at the rear, these axles were combined to form a single rigid body.

The vehicle was allowed to translate longitudinally and laterally, and could yaw. The sprung mass rotated about a horizontal roll axis fixed in the unsprung masses, the location of the roll axis being dependent on the kinematic properties of the front and rear suspensions. The unsprung masses also had a roll degree of freedom, enabling the effect of the vertical compliance of the tyres on the roll performance to be included in the model.

The suspension springs, dampers and anti-roll bars generated moments between the sprung and unsprung masses in response to roll motions. The roll stiffness and damping of the vehicle suspension systems were assumed to be constant for the range of roll motions considered. The active roll control systems at each axle consisted of a pair of actuators and a stiff anti-roll bar in parallel with passive springs and dampers. These roll control systems generated additional (controlled) roll moments between the sprung and unsprung masses.

Initially, a simplified tyre model, where lateral forces varied linearly with slip angle, independent of vertical load, was used. This assumption of linearity is reasonable

for lateral motions of moderate amplitude [16]. The effects of aligning moment, camber thrust, roll steer and rolling resistance generated by the tyres are of secondary importance and were neglected.

The linear model assumed that the forward speed of the vehicle was constant during any lateral manoeuvre. (Although forward speed is an important stability parameter, it is not considered to be a variable of motion.)

The equations of motion for the linear single unit vehicle model are given in appendix A (shown as ordinary differential equations (A1)–(A5), and in state space form in equations (A6)–(A12)). The state space equation is of the form

$$\dot{x} = Ax + B_0u + B_1\delta \quad (1)$$

where x is the state vector, u is a vector of control torques at the active anti-roll bars and δ is the input steering angle. Nomenclature is detailed in appendix B.

Some simulations were performed in the time domain using a nonlinear model. The primary source of nonlinearity is the variation of tyre cornering stiffness F_y/α with vertical load F_z , and this variation can be described using the quadratic equation

$$\frac{F_y}{\alpha} = c_1 \times F_z + c_2 \times F_z^2 \quad (2)$$

where c_1 and c_2 are constants. This equation is generally suitable for lateral accelerations up to the roll-over point and is widely used in heavy vehicle simulation studies [6].

2.1.2 Flexible frame model

The model presented in section 2.1.1 assumed that the vehicle frame was a rigid body. Previous investigations into the use of active roll control systems on heavy vehicles have all used this assumption. However, torsional compliance of the vehicle frame influences the distribution of roll moments between axle groups, and significant frame

compliance affects roll and handling performance noticeably. Winkler et al. noted that “the torsional compliance of the vehicle frame stands out as a uniquely important element in establishing the roll stability of some vehicles, particularly those with flat-bed trailers” [19]. It is essential to include the torsional flexibility of the frame in the vehicle model to predict the roll-over threshold of such vehicles accurately.

Since the motivation for including the frame flexibility was only to capture the influence of compliance on the distribution of roll moments between axles (and not to model torsional vibration), a simple model of the frame using two rigid bodies was used. The sprung mass was split into front and rear sections, each with appropriate inertial properties. These two sections of the sprung mass were connected with a torsional spring whose stiffness matched the torsional stiffness of the vehicle frame. The torsional spring was sited at the centroid height of the frame, so that the line of action of the lateral shear force in the vehicle frame was properly represented. A small amount of torsional damping, representing the energy dissipation inherent in the structure of the vehicle frame, was also included. The incorporation of frame torsional flexibility introduced an additional degree of freedom and an additional equation of motion to the model described in section 2.1.1.

2.2 Linear multiple unit vehicle model

Linear models of multiple unit articulated heavy vehicles can be assembled using modified versions of the single unit equations of motion presented in section 2.1 (see [14] for details). The modifications are necessary to account for the forces and moments applied between adjacent vehicle units through the couplings. An additional equation to describe the kinematic constraint between adjacent vehicle units is required at each coupling. In this way, models of tractor semi-trailers, truck full-trailers and other long combination vehicles can be derived. Figure 2 shows the model used to investigate the performance of a tractor semi-trailer. It had nine degrees of freedom: the five degrees of freedom of the tractor unit (yaw, sideslip, sprung mass roll angle, steer axle roll an-

gle and drive axle roll angle), plus the articulation angle between the tractor and trailer, the front and rear roll angles of the sprung section of the trailer, and the roll angle of the trailer axle group.

2.3 Active roll control system model

The active roll control system at an axle group generates a roll moment between the sprung and unsprung masses in response to a demand signal from the controller. Figure 3 shows how the dynamics of the roll control system (as described by the transfer function G_{arcs} from the moment demanded to the moment generated) affect the closed-loop dynamics of the controlled vehicle.

3 Achievable roll stability

3.1 The roll-over threshold

For a vehicle travelling on a level, paved highway, the main inputs that can cause roll-over are the lateral forces on the tyres during cornering. The effects of cross winds, excessive road camber and irregularities in the road surface are of secondary importance and are neglected here.

The accepted method for static quantifying roll stability is to use the *roll-over threshold*, which is the limit of steady-state lateral acceleration that a vehicle can sustain without losing roll stability.

Accident statistics for heavy vehicles show a strong correlation between low static roll stability (that is, low roll-over threshold) and the likelihood of being involved in a roll-over accident [16]. Although it is clear that both static and dynamic effects influence roll stability, a steady-state analysis of the roll stability gives useful insight into the major elements governing the roll response of the vehicle.

3.2 Mechanics of roll-over

The fundamental mechanics of the roll-over process can be investigated using simplified vehicle models.

3.2.1 Simplified suspended vehicle

First consider a vehicle suspended on compliant passive suspensions and tyres, as shown in figure 4. Initially it is convenient to assume that the total mass of the vehicle is in the sprung mass, that the compliance of the suspensions and tyres is lumped into a single equivalent compliance, and that the roll of the sprung mass on the tyres and suspension springs takes place about the point on the ground plane at the mid-track position [16].

The lateral tyre forces generated at the ground during cornering produce a steady-

state lateral acceleration of the vehicle. Taking moments about the point on the ground plane at the mid-track position gives

$$ma_y h_{cm} = \Delta F_z T - mgh_{cm}\phi. \quad (3)$$

where

- (i) the *primary overturning moment*, $ma_y h_{cm}$, is due to the lateral acceleration,
- (ii) the *restoring moment*, $\Delta F_z T$, arises from the lateral load transfer from the inside tyres to the outside tyres,
- (iii) the *lateral displacement moment*, $mgh_{cm}\phi$, is a consequence of the roll motion which displaces the centre of mass laterally from the nominal centre line of the vehicle.

The primary overturning moment is a destabilising moment, and the vehicle will be unstable in roll whenever this moment exceeds the net stabilising moment that can be provided by the vehicle. For this reason, *the analysis of the roll stability of heavy vehicles focuses on the ability of the vehicle to provide a stabilising moment.*

The suspension can only generate a moment by some rolling of the sprung mass. The restoring moment increases linearly with roll angle up to a maximum value of $\frac{1}{2}mgT$. The roll-over threshold is then

$$a_y = \frac{Tg}{2h_{cm}} - \phi^*g \quad (4)$$

where ϕ^* is the critical roll angle at wheel lift-off. The roll-over threshold is reduced by increasing the roll compliance of the tyres and suspension because stiffer suspensions and tyres cause the lateral displacement moment at wheel lift-off to decrease.

In reality, the sprung mass rolls about a suspension roll centre that is not at ground level, as shown in figure 4. The position of the roll centre is determined by the suspension geometry and is generally some distance above the road surface. The unsprung

mass rotates about a separate roll centre in the ground plane. In general, a higher roll centre will promote less body roll (and correspondingly less lateral displacement of the centre of gravity) and more tyre roll. Since the tyres are significantly less compliant in roll than the suspensions, increasing the suspension roll centre height will typically increase the overall roll stability of the vehicle.

3.2.2 Suspended vehicle with multiple axles

To extend the discussion of the mechanics of roll-over further, consider a vehicle suspended on multiple compliant suspensions and tyres.

The balance between the primary overturning moment and the net restoring moment can be represented on a *roll response graph*, as shown in figure 5. This graph is a useful tool for understanding the roll stability of heavy vehicles [16]. The primary overturning moment is plotted against lateral acceleration on the left side of the graph. The *net restoring moment*, which is the sum of the restoring moment and the lateral displacement moment, is plotted against roll angle on the right side of the graph.

In this example, the trailer axle has the highest stiffness-to-load ratio, followed by the tractor drive axle and the tractor steer axle. The trailer axle group is also the most heavily laden, again followed by the tractor drive axle and the tractor steer axle.

For a given track width, the more heavily laden the axle, the greater the maximum restoring moment it can provide. Thus the maximum suspension moment that can be supplied is higher for the trailer axle group (point *A*) than for the tractor drive axle (*B*) or the tractor steer axle (*C*).

The roll angle at wheel lift-off for a given axle is dictated by the ratio of effective roll stiffness to vertical load, such that axles with a higher stiffness-to-load ratio lift off at smaller roll angles. Thus the roll angle at which the trailer axle group lifts off (*A*) is lower than the corresponding angles for the tractor drive axle (*B*) or the tractor steer axle (*C*).

The net restoring moment is the sum of the suspension moments and the lateral acceleration moment. Up to point *D*, all suspensions contribute a moment proportional

to the body roll angle and the multiple axle vehicle model behaves identically to the simplified model in section 3.2.1. At point D , the inside tyres of the trailer axle group lift off. The slope of the net restoring moment is reduced beyond D because the trailer axles can not provide any additional moment. At point E , the inside tyres of the tractor drive axle lift off. The slope of the net restoring moment curve decreases again beyond E . Since the tractor steer axle is not sufficiently stiff to provide a restoring moment to balance the lateral displacement moment, the roll-over threshold of the vehicle is defined by the lift off of the inside wheel of the tractor drive axle (E) rather than of the steer axle (F).

Figure 5 shows that the non-uniformity of the stiffness-to-load ratios and the resulting non-simultaneous wheel lift-offs reduce the roll-over threshold from the value at point G which would be computed using the lumped suspension model presented in section 3.2.1.

It is clear that the distribution of roll stiffness among the suspensions has an important influence on the roll-over threshold.

An increase in the roll stiffness of the trailer suspension will shift the trailer lift-off point (D) to the left on the roll response graph but will not affect the vehicle roll-over threshold. A decrease in the roll stiffness of the trailer axle will decrease the roll-over threshold only if the stiffness-to-load ratio of the trailer axle is reduced below that of the tractor drive axle, such that the inside wheel of the tractor drive axle lifts off before the inside wheel of the trailer axle.

A change in the roll stiffness of the tractor drive axle will directly affect the roll-over threshold, since the lift-off of the inside wheel of the tractor drive axle defines the roll-over condition for this vehicle. Increasing the roll-over stiffness of the tractor drive axle will increase the roll-over threshold (moving B to the left and E up and to the left).

The roll-over threshold can also be increased by increasing the stiffness of the tractor steer axle. If the steer axle is stiffened to the point where the positive slope of the steer axle roll moment curve is steeper than the negative slope of the lateral

displacement moment curve, then the roll-over threshold of the vehicle will be determined by the lift-off of the inside wheel of the tractor steer axle (F) not the tractor drive axle (E). This is not normally possible in practice.

3.2.3 Other factors influencing roll stability

Suspension lash, present in the leaf spring suspension systems commonly used on heavy vehicles, degrades the roll-over threshold by reducing the effective roll stiffness of the suspensions.

Torsional compliance of the vehicle frames also reduces the roll-over threshold. For example, a flexible trailer frame rolls to a greater angle under the influence of lateral acceleration, thus increasing the magnitude of the destabilising lateral displacement moment. Furthermore torsional compliance of the tractor frame reduces the ability of the tractor steer axle to provide a stabilising moment to resist the roll motion of the payload.

Torsional compliance of the vehicle couplings reduces roll stability in a similar way. Note that the roll stiffness of a conventional fifth wheel coupling decreases with articulation angle, and the roll moment that can be transmitted through a fifth wheel coupling saturates at an included angle of around 2° .

Winkler et al. noted that most real world roll-over accidents feature some dynamic component that raises the vehicle's centre of mass a small distance through its apex height after all axles have left the ground [19]. Cooperrider et al. investigated the energy required for dynamic roll-over and concluded that the lateral acceleration required to achieve roll-over in the dynamic case is slightly higher than the static roll-over threshold [4].

3.3 Controllability analysis

The objective of the roll control system is to use roll moments from active anti-roll bars to maximise the roll stability of the vehicle. Roll stability is achieved by limiting

the lateral load transfers

$$\Delta F_z = \frac{k_t \phi_t}{T} \quad (5)$$

to below the levels required for wheel lift-off. While attempting to minimise load transfers, it is also necessary to constrain the roll angles between the sprung and unsprung masses ($\phi - \phi_t$) to be within the limits of travel of the suspensions. A maximum suspension roll angle of 6-7° is typical.

3.3.1 System model

The vehicle is cast as a multiple input multiple output (MIMO) plant with a series of inputs, internal states and outputs. The *inputs* are external disturbances (steering input δ from the driver) and control inputs. The control inputs are roll moments u between the sprung and unsprung masses generated by active anti-roll bars sited at some or all of the axles. The *internal states* x could be, for example, the state variables used in the models in section 2, although other combinations are also possible. The *performance outputs* z are combinations of the vehicle states that are to be controlled in some way.

The input-output dynamics are given by

$$\dot{x} = Ax + B_0 u + B_1 \delta, \quad z = C_1 x. \quad (6)$$

3.3.2 Input-output controllability

The question of how well it is possible to control the roll motion of a heavy vehicle using active anti-roll bars is essentially a question of *input-output controllability analysis*. This can be defined as the ability to regulate outputs within specified bounds from their references, in spite of unknown but bounded variations (such as disturbances and plant changes), using the available inputs and measurements [17].

As applied to the roll control of heavy vehicles, input-output controllability refers to the ability to use torques generated by active anti-roll bars to regulate lateral load transfers and roll motions, thereby increasing roll stability. Roll stability should be

maintained despite steering inputs from the driver, variations in vehicle response characteristics from the nominal vehicle model and noise in measurements from sensors.

Controllability is independent of the controller and is a property of the plant (in this case the vehicle) only. Controllability can only be affected by plant design changes. These may include changing the properties of vehicle components, relocating sensors and actuators, adding sensors and actuators or even changing or relaxing the control objectives.

The notion of input-output controllability is a broader and more practical notion of controllability than *state controllability* or *functional controllability*. State controllability describes the ability to bring a system from a given initial state to any final state within a finite time, but gives no regard to either the quality of response between or after these two states or the size of the control inputs required [7]. Functional controllability quantifies the number of plant outputs that can be controlled independently and thus the number of control objectives that can be satisfied simultaneously, and is a necessary condition for input-output controllability [13].

Given the wide range of mathematical methods available for control system analysis and design, it is perhaps surprising that the methods commonly used for input-output controllability analysis are largely qualitative [17].

The most common method is to evaluate performance by exhaustive simulations. However this requires a specific controller design and specific values of disturbances and set points. The key disadvantage of this approach is that it is not possible to know if the apparent controllability limits are a fundamental property of the plant or if they are dependent on the controller designs, disturbances and set points used in the simulations.

A more rigorous approach to input-output controllability analysis is to describe mathematically the control objectives, the class of disturbances and the model uncertainty, and then to synthesize controllers to see whether the objectives can be met. However this approach is difficult and time consuming, particularly when there are a large number of candidate actuators and measurements [17].

A two part input-output controllability analysis is presented in the following section. First, the notion of functional controllability is used to determine the maximum number of control objectives that may be satisfied using a given arrangement of active anti-roll bars. Second, the mechanisms for roll stabilisation at high levels of lateral acceleration are examined in detail to understand the trade-offs between the different control objectives of minimising lateral load transfers and limiting roll angles. This allows decisions about actuator placement, sensor placement and the key control objectives to be made *a priori*, without having to perform a detailed controller design. It also allows the limits to achievable roll stability to be quantified.

3.3.3 Functional controllability analysis

An m input l output system $G(s)$ is functionally controllable if the normal rank of $G(s)$, r , is equal to the number of outputs, that is, if $G(s)$ has full row rank. The system is functionally uncontrollable if $r < l$ [17]. This can happen if the system (1) is input deficient; (2) is output deficient; or, (3) has fewer states than outputs. Functional controllability is generally a structural property of a system, that is it does not depend on specific parameter values. A typical example of a system that is functionally uncontrollable is one with fewer inputs than outputs. Another example is a system where none of the inputs affects a particular output.

The roll moment generated by each active anti-roll bar (or group of active anti-roll bars on a multi-axle suspension group) represents a single control input to the active roll control system. Each axle group also contributes a single output in the form of an unsprung mass roll angle (or equivalently a lateral load transfer, by equation (5)) to the vehicle roll control system. In addition, each vehicle unit contributes either one or two outputs in the form of one or two sprung mass roll angles to the roll control system. Torsionally rigid units contribute one output each, while torsionally flexible units contribute two outputs (one per axle group).

For example a tractor semi-trailer combination with a flexible tractor frame will have six roll outputs: the tractor front roll angle, tractor rear roll angle, trailer roll

angle, and the load transfers at the tractor steer axle, tractor drive axle and trailer axle group). This vehicle has three roll control inputs (the active anti-roll bar roll moments at the tractor steer axle, the tractor drive axle and the trailer axle group).

Such systems are clearly input deficient, that is, there are not sufficient inputs to independently control all outputs (roll angles and load transfers). Therefore a specification that requires independent controllability of all roll angles and load transfers is not achievable using active anti-roll bars alone.

A plant that is functionally uncontrollable has $(l - r)$ frequency dependent uncontrollable output directions. For plants that are functionally uncontrollable, it is necessary to decide whether it is acceptable to keep certain output combinations uncontrolled (that is, to relax the control objectives), or if additional actuators are needed to increase the rank of $G(s)$.

Additional hardware to control the torque transmitted between the sprung masses of adjacent vehicle units (by tilting the coupling) or between the front and rear sprung sections of flexible vehicle units (by twisting the vehicle frame) could be fitted to increase the rank of $G(s)$ and reduce the plant input deficiency. However the practicality of such systems is questionable. Furthermore it would not be possible to completely eliminate the plant input deficiency using this method, so clearly some judicious relaxation of the control objectives is necessary.

To demonstrate how the requirement for functional controllability compromises the ability to meet the preliminary control objectives, consider the simple case of a single unit vehicle with a torsionally rigid frame. Such a vehicle has two roll control inputs (one each at the steer and drive axles) and three roll-plane degrees of freedom (the sprung mass roll angle and the lateral load transfers at the steer and drive axles). The following are possible selections for the two controllable roll outputs:

- (i) Control the sprung mass roll angle and the load transfer at the drive axle. The load transfer at the steer axle could not then be specified independently.
- (ii) Control the load transfers at the steer and drive axles. The sprung mass roll angle

could not then be independently specified.

- (iii) Control the sprung mass roll angle and the balance of load transfers between the steer and drive axles. For example, set the normalized load transfers at the steer and drive axles to be the same, so that both axles lift off simultaneously at the roll-over threshold. The total load transfer could not then be independently specified.

3.3.4 Computing inputs and self-regulating outputs

For a functionally controllable plant, it is possible to compute the control inputs required to meet certain control objectives. Consider a vehicle in a steady-state cornering manoeuvre ($\dot{x} = 0$) under a constant steering input δ . The vehicle is fitted with m active anti-roll bars and is required to track m roll control objectives. The required anti-roll bar torques u can be computed if the system is functionally controllable. A modified version of the full state-space model described by equation (A6) is used, with the steering input δ and the active anti-roll bar torques u stacked to form a single input vector. The state vector x is partitioned into three parts: the handling states x_h , the controllable roll states $x_{r,c}$ and the uncontrollable roll states $x_{r,u}$. The matrices A and $B = \left[B_1 \mid B_0 \right]$ are partitioned correspondingly. The aim is to find active roll moments u to meet the control objectives $x_{r,c}$ such that

$$\begin{bmatrix} A_{11} & A_{12} & A_{13} \\ A_{21} & A_{22} & A_{23} \\ A_{31} & A_{32} & A_{33} \end{bmatrix} \begin{bmatrix} x_h \\ x_{r,c} \\ x_{r,u} \end{bmatrix} + \begin{bmatrix} B_{11} & B_{12} \\ B_{21} & B_{22} \\ B_{31} & B_{32} \end{bmatrix} \begin{bmatrix} \delta \\ u \end{bmatrix} = \begin{bmatrix} 0 \\ 0 \\ 0 \end{bmatrix}. \quad (7)$$

The active anti-roll bar torques u have no effect on the steady state handling performance of the linearised system, that is, $A_{12} = A_{13} = B_{12} = 0$. Equation (7) can therefore be rewritten as

$$0 = A_{11}x_h + B_{11}\delta, \quad (8)$$

$$0 = A_{21}x_h + A_{22}x_{r,c} + A_{23}x_{r,u} + B_{21}\delta + B_{22}u, \quad (9)$$

$$0 = A_{31}x_h + A_{32}x_{r,c} + A_{33}x_{r,u} + B_{31}\delta + B_{32}u. \quad (10)$$

Rearranging equation (8) gives an expression for the handling states x_h in terms of the steering input δ :

$$x_h = -A_{11}^{-1}B_{11}\delta. \quad (11)$$

Combining equations (9) and (10) to eliminate the terms in the uncontrollable roll states $x_{r,u}$ and then replacing terms in x_h with terms in δ using equation (11) gives a one-to-one mapping between the controllable roll states $x_{r,c}$ and the control inputs u , of the form

$$u = K_c x_{r,c} + K_\delta \delta \quad (12)$$

where K_c and K_δ are constant matrices depending on the vehicle parameters:

$$K_c = \left(B_{22} - A_{23}A_{33}^{-1}B_{32} \right)^{-1} \left(A_{23}A_{33}^{-1}A_{32} - A_{22} \right), \quad (13)$$

$$K_\delta = \left(B_{22} - A_{23}A_{33}^{-1}B_{32} \right)^{-1} \left[A_{23}A_{33}^{-1} \left(B_{31} - A_{31}A_{11}^{-1}B_{11} \right) - B_{21} + A_{21}A_{11}^{-1}B_{11} \right]. \quad (14)$$

The values of the uncontrollable roll states $x_{r,u}$ can then be solved by back substitution into equation (10).

Since the roll-over threshold depends on both axle lateral load transfers and body roll angles (from section 3.2), the existence of uncontrollable output directions implies that there is a limit to achievable roll stability.

Functional controllability is a necessary but not sufficient condition for input-output controllability. That a system is functionally controllable implies that a set of control of inputs can influence a set of performance outputs *to some extent*. However input-output controllability may still be limited by other factors, including control input saturation, such as occurs at wheel lift-off.

3.3.5 Roll stability and wheel lift-off

The roll response graphs from section 3.2.2 show that the lateral acceleration at which wheel lift-off first occurs is not necessarily a reliable indicator of the roll-over threshold of the vehicle. It is important to establish the conditions under which the vehicle can retain roll stability even when some axles are off the ground and to understand the stabilising mechanisms. The motivation is to identify the *critical* axles, the lift-off of which governs the roll-over threshold.

To investigate the implications of wheel lift-off on vehicle roll stability, consider a linear vehicle model, of the type presented in section 2, but with two modifications:

- (i) The lateral load transfer at each axle is limited to a maximum value determined by the wheel lift-off condition.
- (ii) The roll angle between the sprung and unsprung masses is limited to a maximum value determined by the available suspension travel.

3.3.6 Roll stability without active roll control

First consider the case of a vehicle fitted with a conventional passive suspension system. When all load transfers are sub-critical, at low levels of lateral acceleration, the linearised response of the vehicle is governed by

$$\dot{x} = Ax + B_1\delta \quad (15)$$

where the matrices A and B_1 are formed as in section 2. The stability of the system (both in roll and in handling) can be checked by verifying that the eigenvalues of A all lie in the open left half plane.

If the steering inputs excite a response that causes the wheels at one or more axles to lift off, then equation (15) does not hold since the restoring moment at one or more axles reaches a limit. Beyond lift-off the vehicle response is governed by an equation

of the form

$$\dot{x} = \tilde{A}x + (A - \tilde{A})\tilde{x} + B_1\delta. \quad (16)$$

The matrix \tilde{A} is a modified version of A with the tyre roll stiffness terms k_t set to 0 at the lifted axles. This accounts for the fact that, after lift-off, an axle can no longer provide any additional restoring moment. The constant vector \tilde{x} is a modified version of x with the unsprung mass roll angles ϕ_t at the lifted axles set to the lift-off value ϕ_t^* and all other entries set to zero.

The concept is best explained using the simple example of a single unit rigid vehicle (from section 2.1.1) with maximum lateral load transfer on the rear axle. The matrix A (equation (A10)) is given by

$$A = E^{-1} \begin{bmatrix} * & * & 0 & 0 & 0 & 0 \\ * & * & 0 & 0 & 0 & 0 \\ 0 & * & m_s gh - k_f - k_r & * & k_{t,f} & k_{t,r} \\ * & * & m_{u,f} gh_{u,f} - k_f & * & k_f + k_{t,f} & 0 \\ * & * & m_{u,r} gh_{u,r} - k_r & * & 0 & k_r + k_{t,r} \\ 0 & 0 & 0 & 1 & 0 & 0 \end{bmatrix} \quad (17)$$

where $*$ denotes a non-zero element. The matrix E is from equation (A9). The state vector x is given by

$$x = \left[\beta \quad \dot{\psi} \quad \phi \quad \dot{\phi} \quad \phi_{t,f} \quad \phi_{t,r} \right]^T. \quad (18)$$

After the rear axle reaches the saturation condition, the matrix \tilde{A} is given by

$$\tilde{A} = E^{-1} \begin{bmatrix} * & * & 0 & 0 & 0 & 0 \\ * & * & 0 & 0 & 0 & 0 \\ 0 & * & m_s gh - k_f - k_r & * & k_{t,f} & 0 \\ * & * & m_{u,f} gh_{u,f} - k_f & * & k_f + k_{t,k} & 0 \\ * & * & m_{u,r} gh_{u,r} - k_r & * & 0 & k_r \\ 0 & 0 & 0 & 1 & 0 & 0 \end{bmatrix} \quad (19)$$

and the constant vector \tilde{x} is given by

$$\tilde{x} = \begin{bmatrix} 0 & 0 & 0 & 0 & 0 & \phi_{t,r}^* \end{bmatrix}^T. \quad (20)$$

Since $(A - \tilde{A})\tilde{x}$ is constant, the stability of the system (both in roll and handling) can be checked by verifying that the eigenvalues of \tilde{A} all lie in the open left half plane. Recall that roll stability is determined by the ability of the vehicle to generate an increase in net restoring moment to balance the increase in primary overturning moment caused by an increase in the steering input. For a vehicle with no active roll control system, the change in net restoring moment is the increase in the stabilising roll moment generated by load transfers at the axles minus the destabilising lateral displacement moment generated by the outboard shift of the sprung masses. Thus, for the vehicle to retain roll stability after wheel lift-off, the compliance of the couplings, frames, and tyres and suspensions of the axles remaining on the ground must be sufficiently small that the destabilising effect of the lateral displacement moment does not exceed the stabilising effect of the lateral load transfer.

This analysis can be used to check the stability of the vehicle with any combination of axle groups on or off the ground and provides a technique for identifying which axles must be on the ground for the vehicle to retain roll stability. The roll stability of the vehicle is dependent only on the lateral load transfers at these axles.

3.3.7 Roll stability with active roll control

Next consider the case of a vehicle with an active roll control system. When all load transfers are sub-critical, the linearised response of the vehicle is governed by

$$\dot{x} = Ax + B_0u + B_1\delta \quad (21)$$

where B_0u represents the effect of the roll moments from the active anti-roll bars (see section 2).

Again the roll stability of the vehicle is determined by the ability of the vehicle to generate a net restoring moment to balance the increase in primary overturning moment generated by an increase in steering input. By varying the control torques between the sprung and unsprung masses, the active roll control system can manipulate the axle load transfers and the body roll angles, thus controlling the net stabilising moment. Specifically it is possible to increase the inward lean of the vehicle units, thus using the lateral displacement moment to provide a stabilising effect within the limits of available suspension travel. (This assumes that the vehicle units whose wheels have lifted off are torsionally coupled to the vehicle units whose wheels remain on the ground, or equivalently, that control torques from vehicle units whose axles remain on the ground can influence the roll angles of the vehicle units whose wheels have lifted off.) Clearly, given a sufficient stabilising effect from the lateral displacement moment, it is possible to nullify the destabilising effect of the primary overturning moment and to stabilise the vehicle in roll.

Achievable roll stability is therefore limited by the ability of the active roll control system to provide a sufficient stabilising lateral displacement moment such that the net restoring moment can balance the primary overturning moment. This ability is in turn limited by the maximum allowable suspension deflection. Once the maximum allowable deflection is reached, the stabilising effect is limited to that which would be provided by infinitely stiff suspension springs holding the sprung masses at the maximum inward roll angle. By analogy with the passive case, the stability of the system can be checked by verifying that the eigenvalues of \tilde{A} all lie in the open left half plane. In the active case, \tilde{A} is formed from A by: (1) setting the tyre roll stiffness terms k_t at the lifted axles to 0 (as before); and (2) setting the suspension roll stiffness

terms k at the other axles towards ∞ . For the single unit rigid truck,

$$\tilde{A} = \lim_{k_f \rightarrow \infty} E^{-1} \begin{pmatrix} \begin{bmatrix} * & * & 0 & 0 & 0 & 0 \\ * & * & 0 & 0 & 0 & 0 \\ 0 & * & m_s g h - k_f - k_r & * & k_{t,f} & 0 \\ * & * & m_{u,f} g h_{u,f} - k_f & * & k_f + k_{t,f} & 0 \\ * & * & m_{u,r} g h_{u,r} - k_r & * & 0 & k_r \\ 0 & 0 & 0 & 1 & 0 & 0 \end{bmatrix} \end{pmatrix}. \quad (22)$$

Even if the axles on the ground provide sufficient moment to tilt the vehicle units into the turn at the maximum allowable angle, the vehicle will still be unstable after wheel lift-off if the compliance of the couplings, frames and tyres of the axles remaining on the ground is sufficiently large that the destabilising effect of the lateral displacement moment exceeds the stabilising effect of the lateral load transfer.

The roll stability of a vehicle may not depend on the lateral load transfers at *all* axles. If there is excessive torsional compliance in vehicle frames, couplings or tyres, then it is possible for one section of a combination vehicle to lose roll stability while the lateral load transfers at other axles remain sub-critical.

It is important to control the lateral load transfers at these sub-critical axles, since the control system cannot stabilise the vehicle once the lateral load transfers at these axles reach the critical value required for wheel lift-off.

3.3.8 Roll moment distribution to maximise the roll-over threshold of a tractor semi-trailer

The functional controllability analysis in section 3.3.3 demonstrates that it is not possible to control simultaneously and independently all axle load transfers and body roll angles. It is necessary to identify the vehicle state (that is, the load transfers and roll angles at each axle for a given lateral acceleration) that maximises the net restoring moment and thus maximises the roll stability of the vehicle.

The net restoring moment is equal to the sum of the restoring moments at the axles due to lateral load transfer plus the sum of the stabilising moments due to the lateral displacements of the sprung masses. Since in general it is not possible to simultaneously maximise these two quantities, some compromise is required. Two alternative options for maximising the roll-over threshold of a tractor semi-trailer are now presented.

The example that will be used to illustrate these concepts is the tractor semi-trailer model (see section 2.2). In this case, the tractor frame was assumed to be torsionally rigid. Therefore the vehicle has five roll states (the sprung mass roll angles of the tractor and semi-trailer, and the lateral load transfers at the tractor steer axle, the tractor drive axle and the semi-trailer axles) and three controllable active anti-roll bar torques (one at each of the three axle groups).

Case I: Maximising restoring moment from the axles

The first option is to set the restoring moment of all axles to the maximum possible load transfer (which corresponds to their value at roll-over). The steady-state roll angle and normalised lateral load transfer* responses of a tractor semi-trailer employing such a control scheme are shown in figure 6.

The load transfer specification forms a full set of functionally controllable states $x_{r,c}$ in equation (7). It is not possible to specify any of the sprung mass roll angles independently, but instead the sprung mass roll angles required to achieve this specification are dependent states $x_{r,u}$ that are a function of the steering input.

At low levels of lateral acceleration, this strategy requires that the vehicle is tilted *out* of the the turn, which is clearly undesirable in practice.

For lateral accelerations below 0.45 g, it is not possible to lean this particular vehicle out of the turn enough to generate full load transfer at the axles because the semi-trailer suspension reaches its limiting roll angle. At 0.45 g it is possible to generate maximum load transfer at the tractor and semi-trailer axles by tilting the tractor

*The lateral load transfer is normalised such that a value of ± 1 corresponds to the maximum load transfer possible.

out of the turn by 2° and the semi-trailer out of the turn by 6° (see figure 6(a)). As lateral acceleration increases, it is possible to maintain normalised load transfers of 1 by leaning the tractor and semi-trailer progressively into the turn. The maximum allowable lateral acceleration corresponds to the vehicle state where the maximum inward sprung mass roll angle is equal to the maximum allowable roll angle. In this case, the tractor roll angle is 6° into the turn (point *A*), the semi-trailer roll angle is 3.2° into the turn (point *B*) and the lateral acceleration at roll-over is 0.54 g (points *A* and *B*). The relative roll angle between the tractor and semi-trailer reduces the load transfer on the semi-trailer and increases the load transfer on the tractor. Although the restoring moment from the axles is maximised, the stabilising lateral displacement moment is not.

It is possible that all sprung mass roll angles will reach the maximum allowable roll angle simultaneously, in which case the restoring moment and the stabilising lateral displacement moment would be maximised simultaneously. However, in general this will not be the case and the relative roll angles between the sprung masses at roll-over will be non-zero. These relative roll angles are normally needed to allow the total overturning moment to be shared among the axles to meet the control specification.

Case II: Maximising stabilising lateral displacement moment

The second option is to implement a scheme that sets the inward roll angle of the sprung mass at each axle to the maximum allowable roll angle. This maximises the stabilising effect of the lateral displacement moment. The steady-state roll angle and normalised lateral load transfer responses of a tractor semi-trailer employing such a control scheme are shown in figure 7.

The roll angle specification forms a full set of functionally controllable states $x_{r,c}$ in equation (7). It is not possible to specify any of the lateral load transfers independently, but instead the lateral load transfers required to achieve this specification are dependent states $x_{r,u}$ that are functions of the steering input.

At very low levels of lateral acceleration, the inward lean of the tractor and semi-

trailer causes a small inward lateral load transfer. However at modest levels of lateral acceleration (more than approximately 0.05 g) the load transfer is towards the outside of the turn. When the lateral acceleration increases to 0.45 g, load transfer reaches its maximum possible value at the semi-trailer axles (point *D*) while the tractor axles still have significant additional load transfer capacity (point *F*). However the lateral acceleration at which wheel lift-off first occurs is not a reliable indicator of the roll-over threshold (see sections 3.2.2 and 3.3.5) because the vehicle can remain stable with a limited number of axles on the ground, subject to the stability conditions detailed in section 3.3.5.

As the lateral acceleration increases (see figure 6), the roll angle of the semi-trailer can not be maintained at the maximum value, and the roll angle decreases towards point *C*. This is because the wheel lift-off point sets a maximum value of control torque that can be generated at an axle, so any additional overturning moment must cause a reduction in the inward sprung mass roll angle. Equivalently, since the restoring torque at the lifted axle reaches a maximum at wheel lift-off, then some roll angle outward relative to the adjacent sprung masses is required to provide an additional stabilising torque to balance any additional destabilising overturning moment. Once the semi-trailer axles lift off, the load transfer at the tractor axles increases rapidly until roll stability is lost at 0.54 g (point *E*). By this point the semi-trailer roll angle has been reduced to 3.2° (point *C*).

Significantly, the vehicle states (load transfers and roll angles) at roll-over for the two control schemes described above in case I and case II are identical, and both schemes yield the same roll-over threshold. *The techniques of maximising the restoring moment and maximising the stabilising lateral displacement moment are therefore two different but equivalent ways of maximising the roll-over threshold.* The following equivalent control strategies can therefore be used to maximise the roll stability of the vehicle:

- (i) Balance the normalised load transfers at all critical axles while setting the maximum inward roll angle among the sprung masses to the maximum allowable

angle.

- (ii) Maximise the inward roll angle of the sprung masses.

The first control strategy is preferable for several reasons: (1) actuator force and power requirements are reduced; (2) actuator bandwidth requirements are reduced; (3) the more progressive transition towards roll-over minimises the variation in handling characteristics; and (4) an undesirable sign change in the roll rate response of the semi-trailer is avoided.

The control inputs required to regulate these outputs may or may not include active anti-roll bars at all axle groups. To maximise roll stability, active anti-roll bars need only be fitted at axles from where they can exert some influence on the control outputs[†]. This can be verified by a functional controllability analysis from a reduced set of candidate control inputs to the new set of control outputs.

[†]It may be desirable to modify the control strategy for the steer axle so as to produce acceptable handling performance, possibly at the expense of some degradation of roll-over threshold.

4 Simulation results

In order to demonstrate the achievable improvements to roll stability that can be obtained using active anti-roll bars, roll control systems have been designed and simulated for a range of heavy vehicles [14]. The results for a full-state feedback active roll control system for a tractor semi-trailer are presented here.

4.1 Control system design

The control system design techniques used to design active roll control systems are detailed in full in [14]. The main ideas are as follows.

Since it is desirable to optimise the active roll control system across the range of possible steering inputs rather than simply in response to a single manoeuvre, the control system design problem is one of optimal disturbance rejection, where the disturbance to be rejected is the steering input from the driver.

The problem can be formulated as the synthesis of an optimal linear quadratic regulator in the presence of an exogenous input (the steering). The steering input is described by a shaping filter (A_D, B_D, C_D, D_D) such that a zero-mean white noise source w at the input to the filter produces an appropriately time correlated stochastic steering disturbance δ at the output:

$$\dot{x}_D = A_D x_D + B_D w, \quad \delta = C_D x_D + D_D w. \quad (23)$$

Lin et al. developed a suitable steering spectrum by combining a low frequency steering spectrum from UK road alignment data with a higher frequency steering spectrum to represent lane change manoeuvres [9, 12]. Combining the spectral densities from these low and high frequency sources, he found that, for a very active level of driver input on a typical road, the steering input spectrum could be modelled approximately by

$$S_\delta(\omega) = \frac{0.00014}{\omega^2 + 4} \text{rad}^2/(\text{rad/s}) \quad (24)$$

This corresponds to white noise filtered with a first order filter with a cut-off frequency of 4 rad/s:

$$\dot{x}_D = -4x_D + 2w, \quad \delta = 2x_D. \quad (25)$$

This steering disturbance δ then acts as the input to the vehicle system through the input injection node described by the matrix B_1 such that the dynamics of the system are described by

$$\begin{aligned} \dot{x} &= Ax + B_0u + B_1\delta \\ &= Ax + B_0u + B_1C_Dx_D + B_1D_Dw, \end{aligned} \quad (26)$$

as shown in figure 8(a).

Equation (26) can be rewritten by forming an augmented state vector \underline{x} including the system states x and the disturbance state x_D such that the dynamics of the system are described by

$$\dot{\underline{x}} = \underline{A}\underline{x} + \underline{B}_0u + \underline{B}_1w \quad (27)$$

where

$$\underline{x} = \begin{bmatrix} x \\ x_D \end{bmatrix}, \quad \underline{A} = \begin{bmatrix} A & B_1C_D \\ 0 & A_D \end{bmatrix}, \quad \underline{B}_0 = \begin{bmatrix} B_0 \\ 0 \end{bmatrix}, \quad \underline{B}_1 = \begin{bmatrix} B_1D_D \\ B_D \end{bmatrix}.$$

The optimal control is chosen to minimise the performance index

$$J = \int_0^\infty (z^T Q z + u^T R u) dt \quad (28)$$

where the matrices Q and R are design parameters representing the relative weighting of the performance output trajectory z and the control input u respectively.

The optimal controller is a feedback controller K_{FB} operating on \underline{x} , and the optimal control law is given by

$$u(t) = K_{FB}\underline{x}(t) \quad (29)$$

where

$$K_{FB} = -R^{-1} \underline{B}_0^T S \quad (30)$$

and where S is the solution to the appropriate Riccati equation [14]. The controller configuration is shown in figure 8(b).

Partitioning the feedback controller $K_{FB} = \begin{bmatrix} K_{FB,1} & K_{FB,2} \end{bmatrix}$ such that $K_{FB,1}$ denotes the gain on x and $K_{FB,2}$ denotes the gain on x_D , the closed loop system is described by

$$\begin{bmatrix} \dot{x} \\ \dot{x}_D \end{bmatrix} = \begin{bmatrix} A + B_0 K_{FB,1} & B_1 C_D + B_0 K_{FB,2} \\ 0 & A_D \end{bmatrix} \begin{bmatrix} x \\ x_D \end{bmatrix} + \begin{bmatrix} B_1 D_D \\ B_D \end{bmatrix} w. \quad (31)$$

The term $B_0 K_{FB,2}$ acts as a feedforward control on the disturbance states x_D . This feedforward action reduces the response of the closed loop system to stochastic disturbances. However the stability of the closed loop system is unaffected by this feedforward control since the closed loop eigenvalues of the system are simply the eigenvalues of $A + B_0 K_{FB,1}$ and A_D .

Effective disturbance rejection can be achieved if the dynamic properties of the disturbance are modelled and included in the controller design [8]. For an optimal disturbance rejection law, the states of the disturbance inputs must be measured or estimated such that the feedback of the disturbance states to the controller becomes part of the feedback law.

The weighting matrices Q and R penalise the performance output z and the control input u respectively. In order to simplify the selection of these matrices, the elements of Q are chosen to penalise only the unsprung mass roll angle terms (since the load transfer at an axle is equal to the unsprung mass roll angle multiplied by the effective roll stiffness of the tyres),

$$z = \begin{bmatrix} \phi_{t,f} & \phi_{t,r} \end{bmatrix}^T. \quad (32)$$

The constraint on suspension roll angles is handled implicitly by selecting the elements of R to be sufficiently large to limit the roll moments from the active anti-roll bars,

since excessive roll moments lead to excessive inward roll angles. A useful starting point for selecting the elements of the weighting matrices is to choose Q and R as diagonal matrices

$$Q = \begin{bmatrix} q_1 & 0 \\ 0 & q_2 \end{bmatrix}, \quad q_i = (z_{i,\max})^{-2} \quad (33)$$

and

$$R = \begin{bmatrix} r_1 & 0 \\ 0 & r_2 \end{bmatrix}, \quad r_i = (u_{i,\max})^{-2} \quad (34)$$

where $z_{i,\max}$ and $u_{i,\max}$ are respectively the maximum acceptable values of the i th elements of the performance output vector and control input vector [3]. From this starting point, an iterative design process follows in which the elements of Q and R are tuned to produce a controller with acceptable performance across a range of manoeuvres. The following tuning procedure was used for the vehicle investigated in this paper and for several other configurations [14], and produced good performance with a reasonably limited number of design iterations:

- (i) Adjust the elements of Q and R to tune the steady-state performance of the system such that the normalised load transfers at all critical axles are balanced and the maximum inward suspension roll angle at roll-over is around 4° . Although this may seem conservative, the largest steady-state suspension roll angle should be less than the maximum allowable angle (approximately 5°) to leave space for overshoot in severe transient manoeuvres; otherwise the axles will strike the bump stops.
- (ii) Simulate the performance of the vehicle for a range of severe transient manoeuvres including step steering inputs and lane changes.
- (iii) If the maximum suspension roll angle in response to any critical[‡] transient manoeuvre is greater than the maximum allowable angle, then the step 1 should be

[‡]A manoeuvre is described as *critical* when the size of the steering input is just sufficient to induce roll-over.

repeated with the largest steady-state inward suspension roll angle at roll-over reduced.

- (iv) If the peak normalised load transfer responses among the axles are poorly balanced in severe transient manoeuvres, it is necessary to adjust the elements of Q and R . This will necessarily require a compromise in the steady-state balance. The compromise required is typically small for torsionally rigid single unit vehicles. A greater compromise is required for articulated vehicles, particularly when a high level of rearward amplification is present, for example at high speed or where pintle hitch couplings are used.

4.2 Vehicle description

The tractor semi-trailer combination consists of the two axle tractor joined to a three axle tanker semi-trailer by a fifth wheel coupling. The tractor and semi-trailer parameters, which are detailed in [14], are from an experimental vehicle that is currently being designed and built at the University of Cambridge. The control strategies developed here will be implemented and tested on this prototype vehicle.

The tractor unit has a wheelbase of 3.7 m, with single tyres on the steer axle and dual tyres on the drive axle. The unladen axle weights are 45 kN on the steer axle and 19 kN on the drive axle. The torsional stiffness of the vehicle frame is 629 kN.m/rad.

The three axles of the semi-trailer are spaced evenly at 1.31 m intervals, and the distance from the front axle centreline to the fifth wheel coupling is 6.39 m. Each axle is fitted with wide single tyres. The tanker body is significantly stiffer than the tractor frame, and the combined torsional stiffness of the tanker frame and the fifth wheel coupling is 3000 kN.m/rad. The unladen mass of the semi-trailer is 5420 kg, and the unladen axle weights are 14 kN on each axle. The total mass of the laden semi-trailer is 33220 kg (including 27800 l of water), and the laden axle weights are 80 kN on each axle.

4.3 Steady-state cornering response

The response of a linear model of the torsionally flexible tractor semi-trailer to a steady-state steering input at 60 km/h is shown in figure 9.

Without active roll control, the vehicle rolls out of the corner. The normalised load transfer builds up most quickly at the tractor drive axle and most slowly at the tractor steer axle, although this effect becomes more pronounced as torsional flexibility of the tractor frame increases. The drive axle lifts off at 0.41 g (point *C*), at which point the normalised load transfer at the tractor steer axle is 0.67 (point *A*) and is 0.85 at the semi-trailer axles (point *B*). As lateral acceleration continues to increase, the slopes of the suspension roll angle and normalised load transfer curves increase. The semi-trailer axles lift off at 0.46 g (point *E*), at which point the normalised load transfer at the steer axle is 0.76 (point *D*). Beyond this point, the steer axle is unable to stabilise the vehicle, and roll-over occurs.

With active roll control, the vehicle rolls into the corner. The total roll moment is distributed among the active anti-roll bars so that the normalised load transfers at all axles increase in a balanced fashion with lateral acceleration. This requires a relative roll angle of $4.0^\circ/\text{g}$ between the front and rear sections of the tractor unit (with the front section rolling into the corner more than the rear) and a relative roll angle between the rear section of the tractor unit and the rear section of the semi-trailer of $1.2^\circ/\text{g}$ (with the tractor rolling into the corner more than the semi-trailer). For greater frame flexibilities, the relative roll angles required to balance the normalised load transfers increase. The normalised load transfers at all axles reach the critical value of 1 simultaneously at 0.60 g (point *F*), at which point the maximum inward suspension roll angle is 4.0° at the tractor steer axle.

Active roll control increases the roll-over threshold of the torsionally flexible tractor semi-trailer by 29% and the lateral acceleration at which axle lift-off first occurs by 45%. This is a significant improvement in steady-state roll stability.

4.4 Response to a step steering input

The response of the vehicle model to a step steering input is shown in figure 10. The step input is scaled to give a maximum normalised load transfer of 1 for the passive vehicle and the steady-state lateral acceleration is 0.41 g.

The suspension roll angle responses are shown in figure 10(a). Without active roll control, the vehicle rolls out of the corner, with peak suspension roll angles of 3.7° at the tractor steer axle and 4.8° at the tractor drive and semi-trailer axles. The active roll control system causes the vehicle to roll into the corner, with peak suspension roll angles of 3.0° at the tractor steer axle, 1.6° at the tractor drive axle and 2.2° at the semi-trailer axles. The corresponding steady-state suspension roll angles are 2.8° , 0.9° and 1.4° . Although the *suspension* roll angle is greater at the semi-trailer axles than at the tractor drive axle, the *absolute* inward roll angle of the tractor's rear section is again actually greater than that of the semi-trailer, the difference being due to the higher stiffness of the tractor tyres.

The normalised load transfer responses are shown in figure 9(b). For the passive suspension, the normalised load transfer again builds up fastest at the tractor drive axle and slowest at the tractor steer axle. This trend is more apparent for more flexible vehicle frames; that is, frame flexibility reduces the ability of the tractor steer axle, in particular, to carry its share of the total lateral load transfer.

The normalised load transfer responses feature small overshoots before settling at final values of 0.67, 1.00 and 0.85 at the tractor steer, tractor drive and semi-trailer axles respectively. In addition to reducing the total lateral load transfer by rolling the vehicle units into the turn, the active roll control system redistributes the load transfer in a balanced fashion among the axles so that all show a peak normalised value of 0.69 at all axles. The system reduces the peak load transfer by 31% at the tractor drive axle and by 19% at the semi-trailer axles. The load transfer at the tractor steer axle remains essentially unchanged. However, rather than indicating poor controller performance, this emphasises that the tractor steer axle carries much less than its "fair share" of the total load transfer in the passive case.

The steady-state results in section 4.3 show that, with passive suspension, the roll-over threshold for this vehicle is 12% higher than the lateral acceleration at which axle lift-off first occurs. However, with active roll control, the vehicle can remain stable with up to 45% additional lateral acceleration (that is, up to 0.60 g). This represents a significant improvement in roll stability. The peak inward suspension roll angle in response to such a critical manoeuvre is 4.3° , which is within the allowable limits.

The active anti-roll bar moment responses are shown in figure 10(c). The peak roll moment in response to a critical manoeuvre is 64 kN.m at the drive axle. The roll moment builds up most quickly at the tractor drive and semi-trailer axles to distribute the total load transfer evenly among the axles throughout the early part of this severe manoeuvre.

4.5 Response to a double lane change steering input

The response of the vehicle to a double lane change steering input at 60 km/h is illustrated in figure 11 (see [14] for the definition of this manoeuvre). The path deviation over a 120 m test section is 5.05 m for the tractor and 5.2 m for the semi-trailer. The peak lateral acceleration is 0.21 g.

The suspension roll angle responses are shown in figure 11(a). The trends discussed in sections 4.3 and 4.4 are again apparent. Active roll control causes the vehicle to roll into the corners, with the tractor unit rolling more towards the inside than the semi-trailer.

The normalised load transfer responses are shown in figure 11(b). In the passive case, the normalised load transfers are unbalanced, with the tractor drive axle bearing significantly more than its share of the total load transfer and the tractor steer axle bearing significantly less than its share. The peak load transfers are 0.28 at the tractor steer axle, 0.48 at the tractor drive axle and 0.43 at the semi-trailer axles. When equipped with the active roll control system, the normalised load transfer responses are better balanced, with peak values of 0.30 at all axles. Peak normalised load transfer is re-

duced by 39% at the tractor drive axle and 31% at the semi-trailer axles.

The peak inward roll angle at the semi-trailer axles in response to a critical double lane change steering input is 5.8° . This is within the available suspension travel.

Figure 11(c) illustrates that the largest active anti-roll moment for this manoeuvre is 22 kN.m at the tractor drive axle. The roll moment in response to a critical double lane change steering input for which roll-over would occur is therefore 73 kN.m.

4.6 Effect on handling performance

The effect of active roll control on the handling performance of the torsionally flexible tractor semi-trailer model at 60 km/h is shown in figure 12. This model included the nonlinear tyre characteristics described in section 2.1.1. The handling responses of both the tractor and semi-trailer are included on the figure because the yaw stability of the combination is determined by the handling characteristics of both vehicle units [16].

First, consider the response of the vehicle without active roll control. At low levels of lateral acceleration, the tractor unit understeers mildly. As lateral acceleration increases, the normalised load transfer builds up more quickly at the drive axle than at the steer axle, an effect that is accentuated by reducing the torsional rigidity of the tractor frame. The handling balance of the tractor changes to mild oversteer by 0.2 g. The tractor oversteers with increasing severity as lateral acceleration builds up. Yaw stability will be lost at high speed and high lateral acceleration if both the tractor and semi-trailer are oversteering [16].

Despite the presence of torsional flexibility in the tractor and semi-trailer frames and in the fifth wheel coupling, the active roll control system balances the build up of normalised load transfer evenly between all the axles. The active roll control system causes the understeer gradient of the tractor to increase with lateral acceleration and also reduces the severity of oversteer at the semi-trailer. As long as the tractor unit understeers, the combination cannot be unstable in yaw [16]. Therefore, the ac-

tive roll control system significantly increases yaw stability at high levels of lateral acceleration.

5 Conclusions

1. Roll-over occurs when a vehicle is unable to provide a stabilising net restoring moment to balance an overturning moment. The mechanics of the roll-over process are complex, and wheel lift-off at a particular axle does not necessarily imply a loss of roll stability of the entire vehicle. A procedure for identifying critical axles whose lift-off determines the roll-over threshold was presented.
2. Functional controllability analysis can be used to verify that a candidate set of active anti-roll bars can exert some degree of control over a given set of roll-plane states (load transfers and roll angles). This has important implications for actuator placement.
3. Achievable roll stability is limited because it is not possible to control all axle load transfers and body roll angles independently using active anti-roll bars alone. The best achievable control objective for maximising roll stability was shown to be setting the normalised load transfers at all critical axles to be equal while taking the largest inward suspension roll angle to the maximum allowable angle.
4. Simulations showed that active roll control systems can increase the roll-over threshold of a torsionally flexible tractor semi-trailer by 29%. Such an improvement in roll stability represents a significant increase in vehicle safety.
5. By distributing the total normalised load transfer among all axles in a balanced fashion, active roll control tends to increase understeer for both units of a typical tractor semi-trailer, thus increasing yaw stability.

Acknowledgements

The authors wish to acknowledge the financial support of the Cambridge Vehicle Dynamics Consortium and the Engineering and Physical Sciences Research Council. At the time of writing, the Cambridge Vehicle Dynamics Consortium consisted of the Cambridge and Cranfield Universities together with the following industrial partners from the European heavy vehicle industry: Tinsley Bridge Ltd, ArvinMeritor, Koni BV, Qinetiq, Pirelli, Shell UK Ltd, Volvo Global Trucks, General Trailers, Firestone Industrial Products, Mektronika Systems and Fluid Power Design. Dr Sampson would like to thank the Cambridge Australia Trust and the Committee of Vice-Chancellors and Principals of the Universities of the United Kingdom for their support.

A Equations of Motion

The equations of motion for the linear torsionally rigid single unit vehicle (figure 1) are

$$m_s h \ddot{\phi} = -mU(\dot{\beta} + \dot{\psi}) + Y_\beta \beta + Y_{\dot{\psi}} \dot{\psi} + Y_\delta \delta, \quad (\text{A1})$$

$$-I_{x'z'} \ddot{\phi} + I_{z'z'} \ddot{\psi} = N_\beta \beta + N_{\dot{\psi}} \dot{\psi} + N_\delta \delta, \quad (\text{A2})$$

$$\begin{aligned} I_{x'x'} \ddot{\phi} - I_{x'z'} \ddot{\psi} &= m_s g h \phi - m_s U h (\dot{\beta} + \dot{\psi}) \\ &\quad - k_f (\phi - \phi_{t,f}) - l_f (\dot{\phi} - \dot{\phi}_{t,f}) + u_f \\ &\quad - k_r (\phi - \phi_{t,r}) - l_r (\dot{\phi} - \dot{\phi}_{t,r}) + u_r, \end{aligned} \quad (\text{A3})$$

$$\begin{aligned} -r (Y_{\beta,f} \beta + Y_{\dot{\psi},f} \dot{\psi} + Y_{\delta,f} \delta) &= m_{u,f} U (h_{u,f} - r) (\dot{\beta} + \dot{\psi}) + k_{t,f} \phi_{t,f} \\ &\quad - m_{u,f} g h_{u,f} \phi_{t,f} - k_f (\phi - \phi_{t,f}) \\ &\quad - l_f (\dot{\phi} - \dot{\phi}_{t,f}) + u_f, \end{aligned} \quad (\text{A4})$$

$$\begin{aligned} -r (Y_{\beta,r} \beta + Y_{\dot{\psi},r} \dot{\psi}) &= m_{u,r} V (h_{u,r} - r) (\dot{\beta} + \dot{\psi}) + k_{t,r} \phi_{t,r} \\ &\quad - m_{u,r} g h_{u,r} \phi_{t,r} - k_r (\phi - \phi_{t,r}) \\ &\quad - l_r (\dot{\phi} - \dot{\phi}_{t,r}) + u_r. \end{aligned} \quad (\text{A5})$$

Equation (A1) is a lateral force balance for the entire vehicle. Equation (A2) is a yaw moment balance for the entire vehicle. Equations (A3) describes the balance of roll moments on the sprung mass. Equations (A4) and (A5) describe the roll motions of the front and rear unsprung masses respectively.

These equations can more conveniently be expressed using a state space representation, which is suitable for linear systems analysis and for numerical integration:

$$\dot{x} = Ax + B_0 u + B_1 \delta \quad (\text{A6})$$

where

$$x = \left[\beta \quad \dot{\psi} \quad \phi \quad \dot{\phi} \quad \phi_{t,f} \quad \phi_{t,r} \right]^T, \quad (\text{A7})$$

$$u = \left[u_f \quad u_r \right]^T, \quad (\text{A8})$$

$$E = \begin{bmatrix} mU & 0 & 0 & m_s h & 0 & 0 \\ 0 & I_{z'z'} & 0 & -I_{x'z'} & 0 & 0 \\ m_s U h & -I_{x'z'} & 0 & I_{x'x'} & -l_f & -l_r \\ -m_{u,f} U (h_{u,f} - r) & 0 & 0 & 0 & -l_f & 0 \\ -m_{u,r} U (h_{u,r} - r) & 0 & 0 & 0 & 0 & -l_r \\ 0 & 0 & 1 & 0 & 0 & 0 \end{bmatrix}, \quad (\text{A9})$$

$$A = E^{-1} \begin{bmatrix} Y_\beta & Y_r - mU & 0 \\ N_\beta & N_{\dot{\psi}} & 0 \\ 0 & -m_s h V & m_s g h - k_f - k_r \\ rY_{\beta,f} & rY_{\dot{\psi},f} + m_{u,f} U (h_{u,f} - r) & m_{u,f} g h_{u,f} - k_f \\ rY_{\beta,r} & rY_{\dot{\psi},r} + m_{u,r} U (h_{u,r} - r) & m_{u,r} g h_{u,r} - k_r \\ 0 & 0 & 0 \\ 0 & 0 & 0 \\ 0 & 0 & 0 \\ -l_f - l_r & k_{t,f} & k_{t,r} \\ -l_f & k_f + k_{t,f} & 0 \\ -l_r & 0 & k_r + k_{t,r} \\ 1 & 0 & 0 \end{bmatrix}, \quad (\text{A10})$$

$$B_0 = E^{-1} \begin{bmatrix} 0 & 0 & 1 & 0 & 1 & 0 \\ 0 & 0 & 1 & 1 & 0 & 0 \end{bmatrix}^T, \quad (\text{A11})$$

$$B_1 = E^{-1} \begin{bmatrix} Y_\delta & N_\delta & 0 & rY_{\delta,f} & 0 & 0 \end{bmatrix}^T. \quad (\text{A12})$$

B Nomenclature

A, B, C, D	state-space matrices
a	longitudinal distance to axle, measured forwards from centre of sprung mass
a'	longitudinal distance to axle, measured forwards from centre of total mass
a_y	lateral acceleration
b	longitudinal distance to articulation point, measured forwards from centre of sprung mass
b'	longitudinal distance to articulation point, measured forwards from centre of total mass
c_1, c_2	tyre cornering stiffness coefficients, in $\frac{F_y}{\alpha} = c_1 \times F_z + c_2 \times F_z^2$
c_α	tyre cornering stiffness, measured at rated vertical tyre load
F_y	lateral tyre force
F_z	vertical tyre force
G	plant transfer function
g	acceleration due to gravity
h_a	height of articulation point, measured upwards from ground
h_{cm}	height of total centre of mass, measured upwards from ground
h_s	height of centre of sprung mass, measured upwards from ground
h_u	height of centre of unsprung mass, measured upwards from ground
$I_{x'x'}$	roll moment of inertia of sprung mass, measured about origin of (x', y', z') coordinate system
$I_{x'z'}$	yaw-roll product of inertia of sprung mass, measured about origin of (x', y', z') coordinate system
$I_{z'z'}$	yaw moment of inertia of total mass, measured about origin of (x', y', z') coordinate system
K	controller transfer function
k	suspension roll stiffness
k_t	tyre roll stiffness
l	suspension roll damping rate
m	total mass
m_s	sprung mass
m_u	unsprung mass
N_β	$\frac{\partial M_z}{\partial \beta} = \sum_j a'_j c_{\alpha,j}$ partial derivative of net tyre yaw moment with respect to sideslip angle

N_δ	$\frac{\partial M_z}{\partial \delta} = -a'_1 c_{\alpha,1}$	partial derivative of net tyre yaw moment with respect to steer angle
$N_{\dot{\psi}}$	$\frac{\partial M_z}{\partial \dot{\psi}} = \sum_j \frac{a'_j{}^2 c_{\alpha,j}}{U}$	partial derivative of net tyre yaw moment with respect to yaw rate
r		height of roll axis, measured upwards from ground
s		Laplace variable
T		track width
U		forward speed
u		active roll torque
x		state vector
x'		longitudinal distance, measured forwards from centre of total mass
y		measurement output
y'		lateral distance, measured to the right from vehicle unit centreline
Y_β	$\frac{\partial F_y}{\partial \beta} = \sum_j c_{\alpha,j}$	partial derivative of net tyre lateral force with respect to sideslip angle
Y_δ	$\frac{\partial F_y}{\partial \delta} = -c_{\alpha,1}$	partial derivative of net tyre lateral force with respect to steer angle
$Y_{\dot{\psi}}$	$\frac{\partial F_y}{\partial \dot{\psi}} = \sum_j \frac{a'_j c_{\alpha,j}}{U}$	partial derivative of net tyre lateral force with respect to yaw rate
z		performance output
z'		vertical distance, measured downwards from roll axis
α		tyre slip angle
β		sideslip angle
δ		steer angle
ϕ		absolute roll angle of sprung mass
ϕ_t		absolute roll angle of unsprung mass
ψ		heading angle
$\dot{\psi}$		yaw rate

Notation

A^T	transpose of A
A^{-1}	inverse of A
\dot{a}	first time derivative of a

\ddot{a} second time derivative of a

Additional subscripts

f front
 i i th vehicle unit, or i th vehicle coupling, counted from front
 j j th axle, counted from front
 r rear

References

- [1] Blower, D. and Pettis, L. Trucks involved in fatal accidents. Codebook 1996. Technical Report UMTRI-98-14, University of Michigan Transportation Research Institute, Ann Arbor, MI, USA, 1998.
- [2] Blower, D. and Pettis, L. Trucks involved in fatal accidents. Codebook 1997. Technical Report UMTRI-99-18, University of Michigan Transportation Research Institute, Ann Arbor, MI, USA, 1999.
- [3] Bryson, A. E. and Ho, Y. C. *Applied Optimal Control*. Blaisdell, Waltham, MA, USA, second edition, 1975.
- [4] Cooperrider, N. K., Thomas, T. M., and Hammoud, S. A. Testing and analysis of vehicle rollover behavior. *SAE Transactions*, 99(900366):518–527, 1990.
- [5] Dunwoody, A. B. and Froese, S. Active roll control of a semi-trailer. *SAE Transactions*, 102(933045):999–1004, 1993.
- [6] Fancher, P. S., Ervin, R. D., Winkler, C. B., and Gillespie, T. D. A factbook of the mechanical properties of the components for single-unit and articulated heavy trucks. Technical Report UMTRI-86-12, University of Michigan Transportation Research Institute, Ann Arbor, MI, USA, 1986.
- [7] Kalman, R. When is a linear control system optimal? *ASME Transactions, Journal of Basic Engineering*, 86:51–60, 1964.
- [8] Lin, C.-F. *Advanced Control Systems Design*. Prentice Hall, Upper Saddle River, NJ, USA, 1994.
- [9] Lin, R. C. *An Investigation of Active Roll Control for Heavy Vehicle Suspensions*. Ph.D. thesis, University of Cambridge, Cambridge, UK, 1994.

- [10] Lin, R. C., Cebon, D., and Cole, D. J. Validation of an articulated vehicle yaw/roll model. Technical Report CUED/C-MECH/TR 53, Department of Engineering, University of Cambridge, Cambridge, UK, 1993.
- [11] Lin, R. C., Cebon, D., and Cole, D. J. Active roll control of articulated vehicles. *Vehicle System Dynamics*, 26(1):17–43, 1996.
- [12] Lin, R. C., Cebon, D., and Cole, D. J. Optimal roll control of a single-unit lorry. *Proc. IMechE, Journal of Automobile Engineering*, 210(1):44–55, 1996.
- [13] Rosenbrock, H. H. *State-Space and Multivariable Theory*. Nelson, London, UK, 1970.
- [14] Sampson, D. J. M. *Active Roll Control of Articulated Heavy Vehicles*. Ph.D. thesis, University of Cambridge, Cambridge, UK, 2000.
- [15] Segel, L. Theoretical prediction and experimental substantiation of the response of an automobile to steering control. *Proc. IMechE, Automotive Division*, pages 310–330, 1956–57.
- [16] Segel, L., editor. *Course on the Mechanics of Heavy-Duty Trucks and Truck Combinations*, Surfers Paradise, Qld, Australia, 1988. University of Michigan Transportation Research Institute.
- [17] Skogestad, S. and Postlethwaite, I. *Multivariable Feedback Control – Analysis and Design*. John Wiley & Sons, Chichester, UK, 1996.
- [18] Von Glasner, E.-Ch. Active safety of commercial vehicles. In *Proc. 2nd International Symposium on Advanced Vehicle Control*, pages 9–14, Tsukuba, Japan, 1994.
- [19] Winkler, C. B., Blower, D., Ervin, R. D., and Chalasani, R. M. *Rollover of Heavy Commercial Vehicles*. SAE, Warrendale, PA, USA, 2000.

- [20] Winkler, C. B., Bogard, S. E., Ervin, R. D., Horsman, A., Blower, D., Mink, C., and Karamihas, S. Evaluation of innovative converter dollies. Technical Report UMTRI-93-47, University of Michigan Transportation Research Institute, Ann Arbor, MI, USA, 1993.

- [21] Winkler, C. B. and Ervin, R. D. On-board estimation of the rollover threshold of tractor semitrailers. In *Proc. 16th IAVSD Symposium on the Dynamics of Vehicles on Roads and Tracks*, pages 540–551, Pretoria, South Africa, 1999.

- [22] Winkler, C. B. and Ervin, R. D. Rollover of heavy commercial vehicles. Technical Report UMTRI-99-19, University of Michigan Transportation Research Institute, Ann Arbor, MI, USA, 1999.

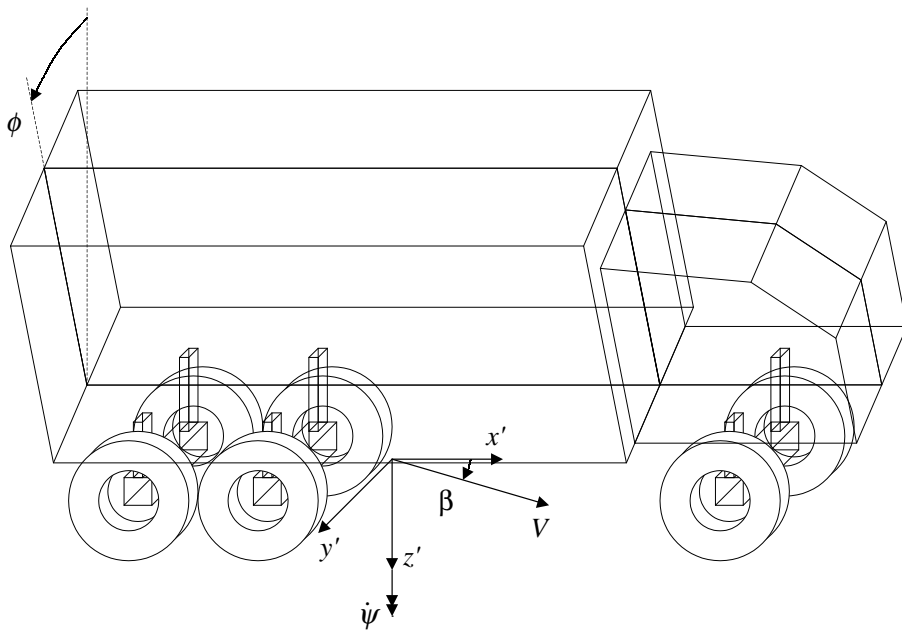


Figure 1: Single unit vehicle with rigid frame (ϕ measured from vertical). The model has five degrees of freedom: yaw rate $\dot{\psi}$, sideslip angle β , sprung mass roll angle ϕ , steer axle roll angle $\phi_{t,f}$, and drive axle roll angle $\phi_{t,r}$.

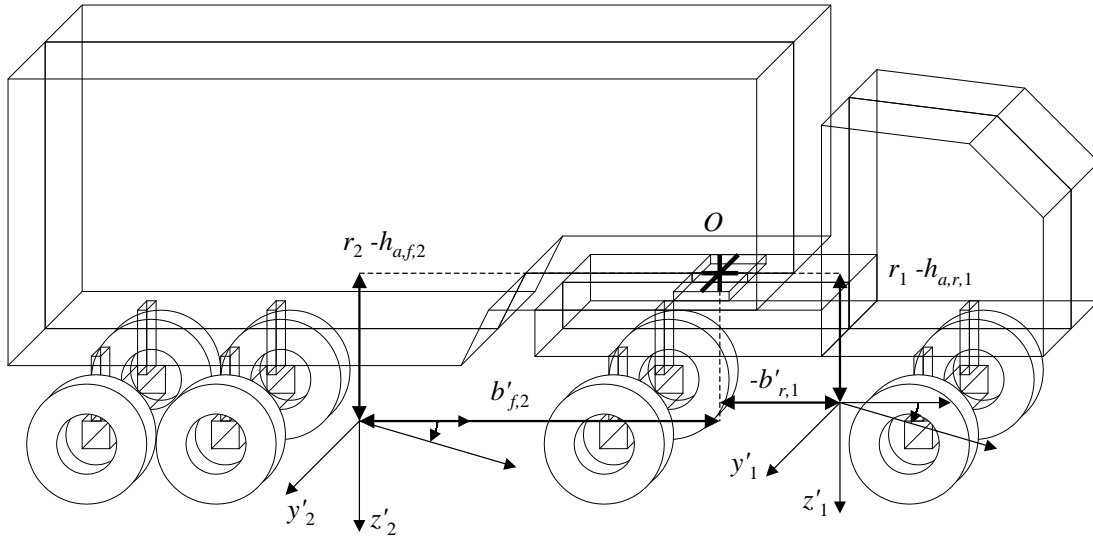


Figure 2: Coordinate systems used to describe the kinematic constraint at vehicle couplings. The model has four degrees of freedom in addition to those listed in figure 1: articulation angle Γ between the tractor and trailer, trailer front and rear sprung mass roll angles $\phi_{f,2}$ and $\phi_{r,2}$, and trailer axle roll angle $\phi_{t,r,2}$.

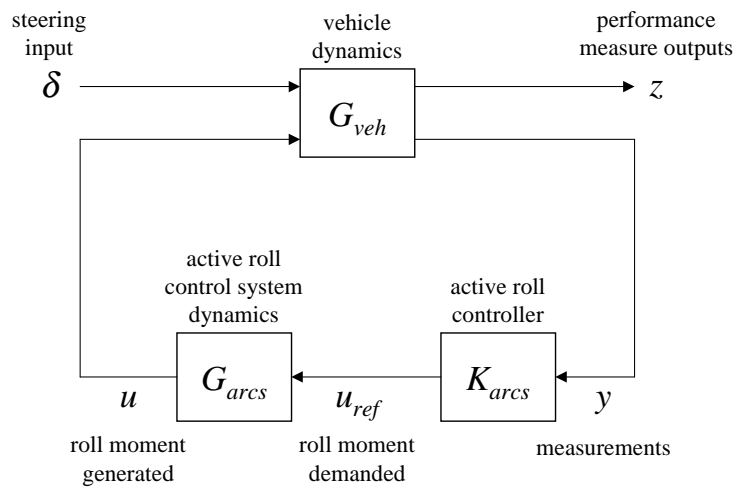


Figure 3: Active roll control system architecture.

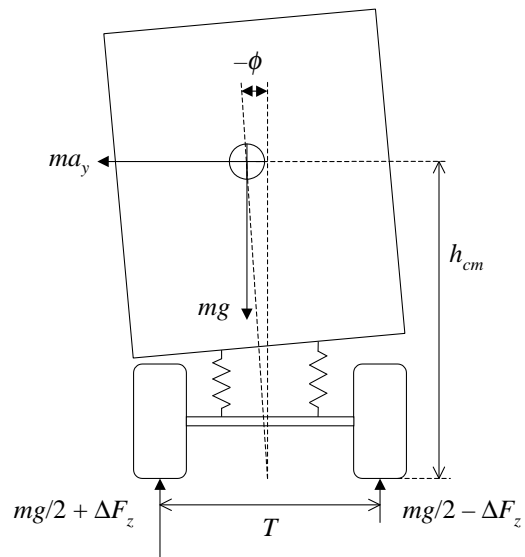


Figure 4: Simplified suspended vehicle model.

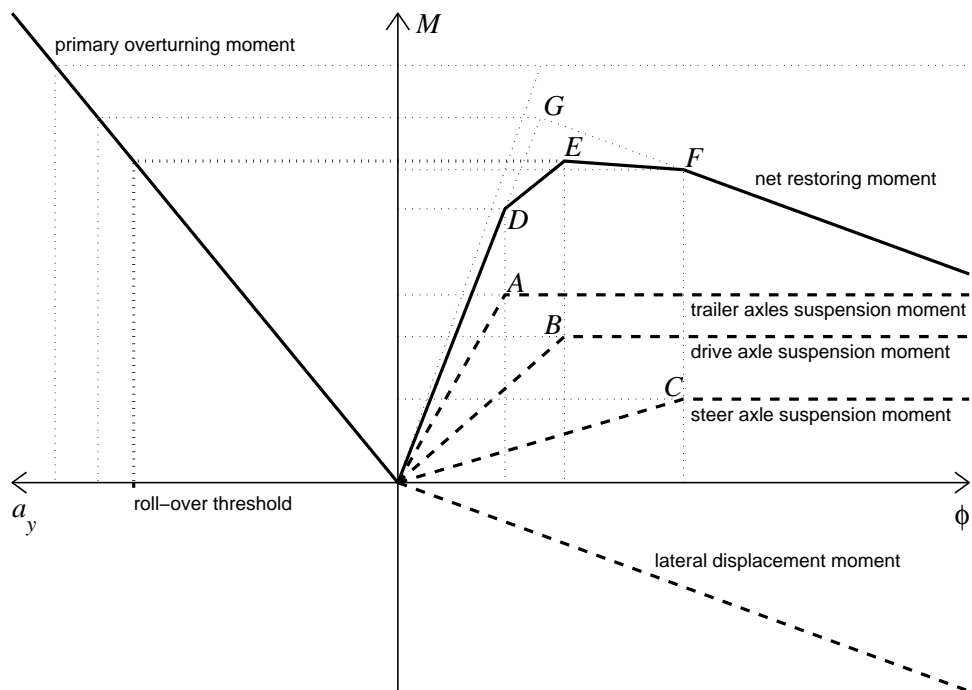
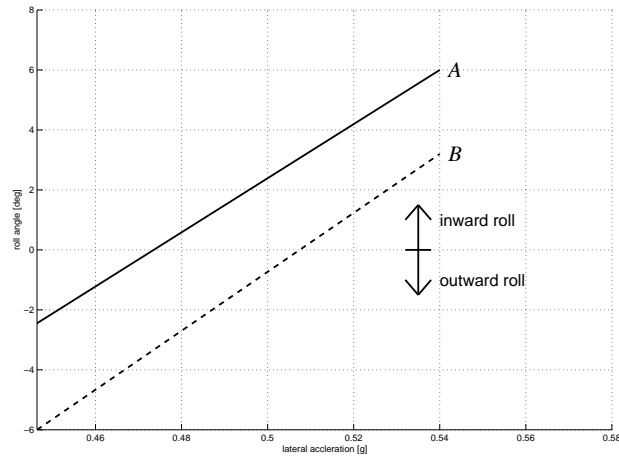
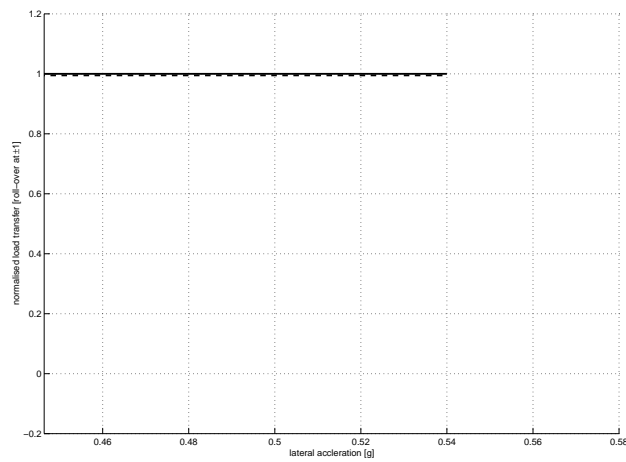


Figure 5: Generic roll response graph for suspended vehicle with multiple axles.

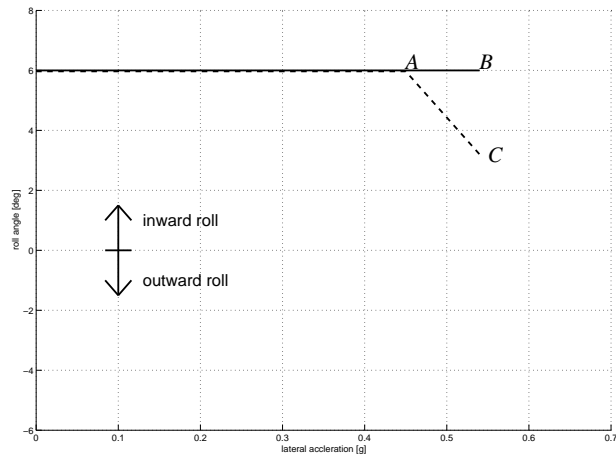


(a) Suspension roll angles. Active roll control: tractor (—), semi-trailer (- - -).

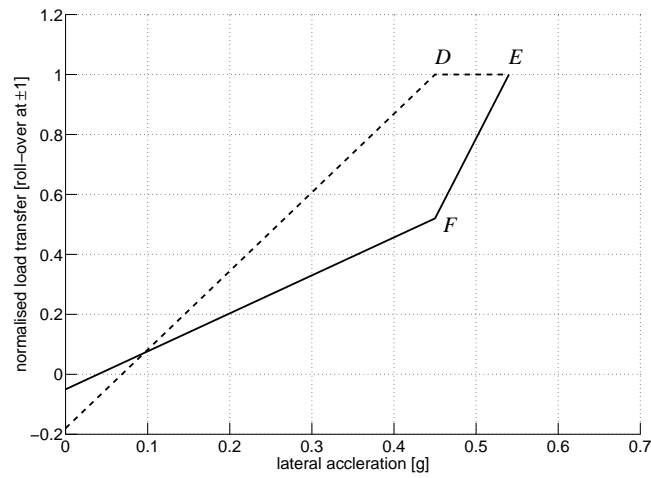


(b) Normalised load transfers. Active roll control: tractor (—), semi-trailer (- - -).

Figure 6: Increasing the roll-over threshold of the tractor semi-trailer by maximising the stabilising axle moment.

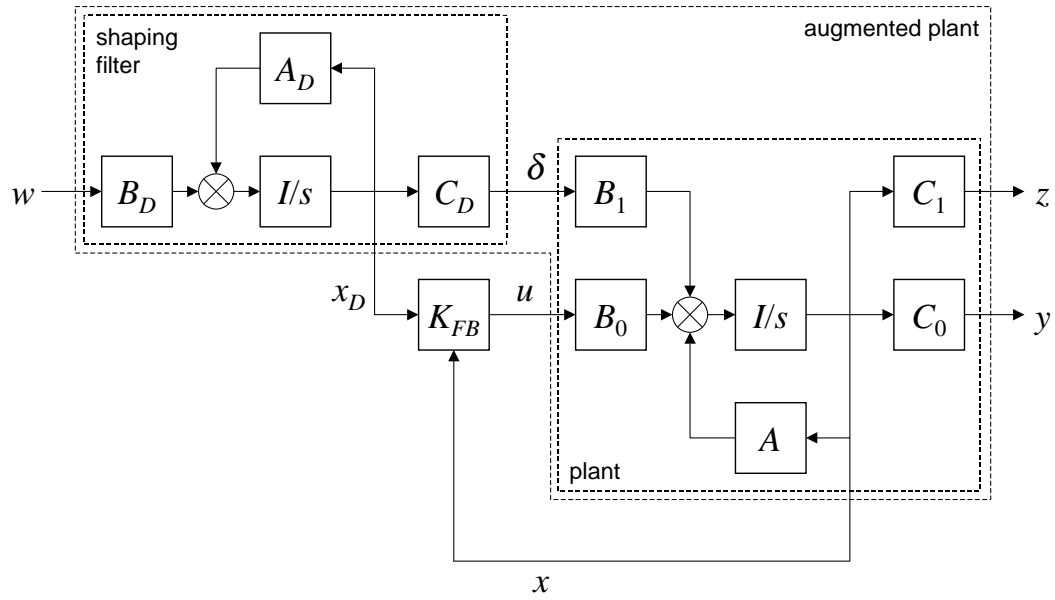


(a) Suspension roll angles. Active roll control: tractor (—), semi-trailer (- - -).

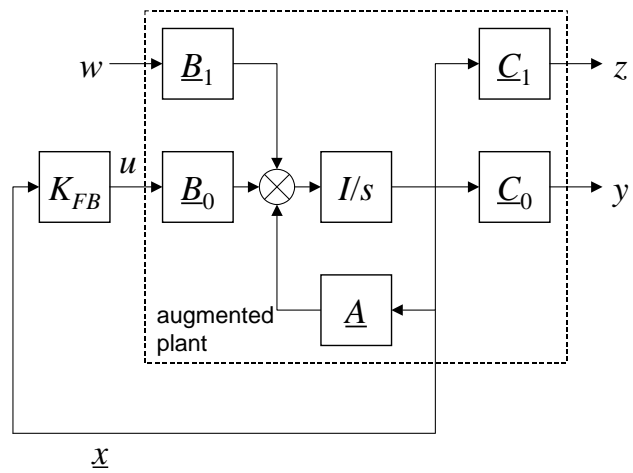


(b) Normalised load transfers. Active roll control: tractor (—), semi-trailer (- - -).

Figure 7: Increasing the roll-over threshold of the tractor semi-trailer by maximising the stabilising lateral displacement moment.

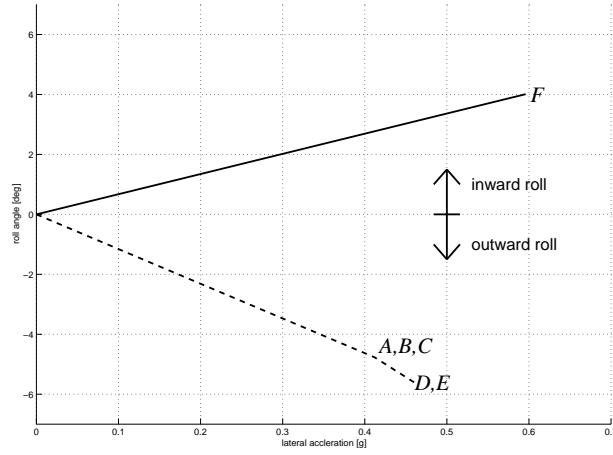


(a) Detailed model showing the shaping filter and the plant.

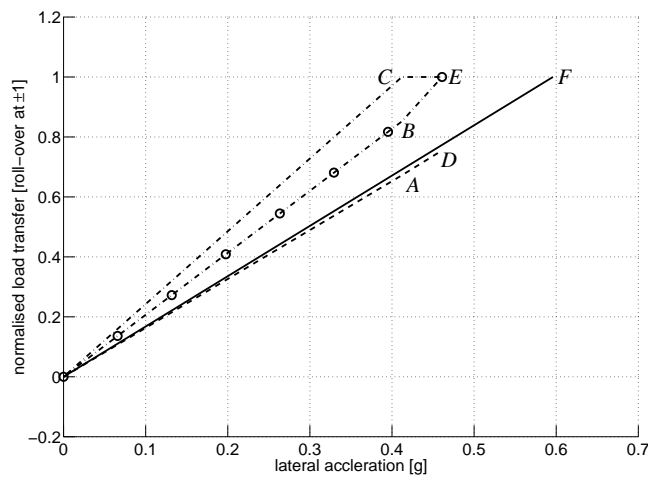


(b) Simplified model showing the augmented plant.

Figure 8: Optimal disturbance rejection.

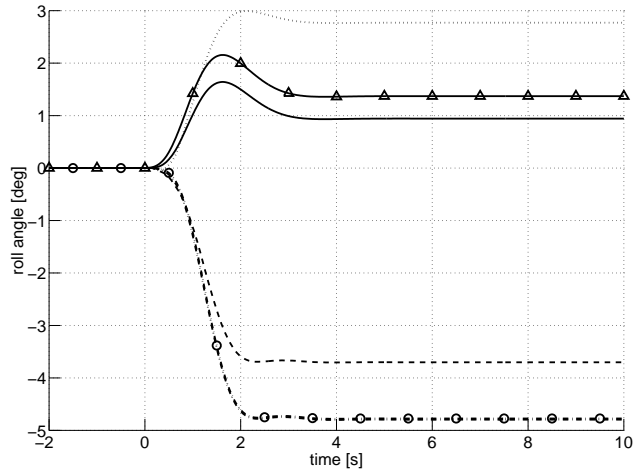


(a) Suspension roll angles. Active roll control: *steer axle* (—); passive suspension: *semi-trailer axles* (- - -).

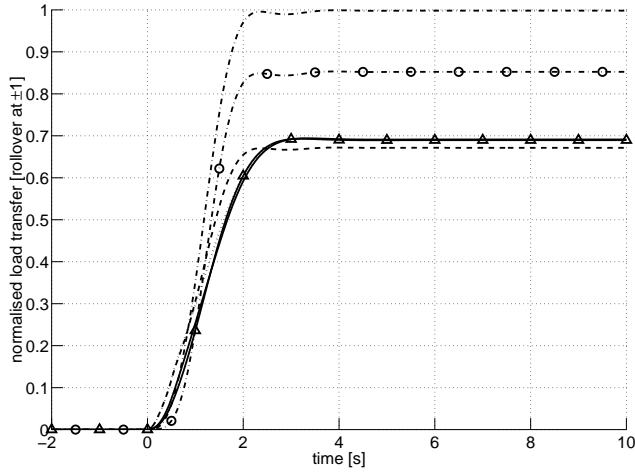


(b) Normalised load transfers. Active roll control: *steer axle, drive axle and semi-trailer axles* (—); passive suspension: *steer axle* (- - -), *drive axle* (· - · - ·) and *semi-trailer axles* (· - ○ - ·).

Figure 9: Response of the linear, torsionally flexible tractor semi-trailer model with a passive suspension or a full-state feedback controller to a steady-state steering input.

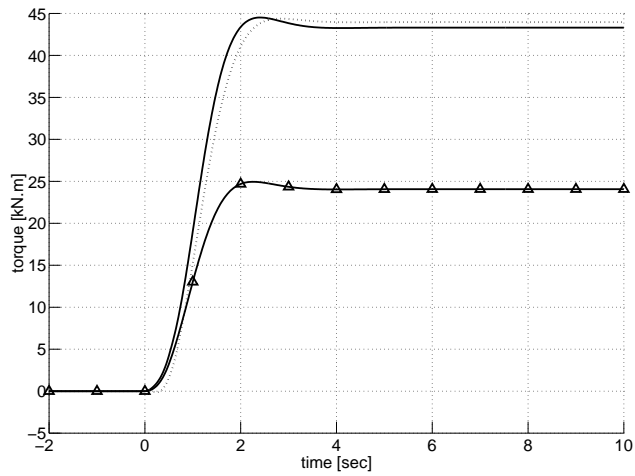


(a) Suspension roll angles. Active roll control: *steer axle* ($\cdots\cdots$), *drive axle* (—), *semi-trailer axles* ($\text{—}\triangle$); passive suspension: *steer axle* (---), *drive axle* ($\cdots\cdots$), *semi-trailer axles* ($\cdots\circ\cdots$).



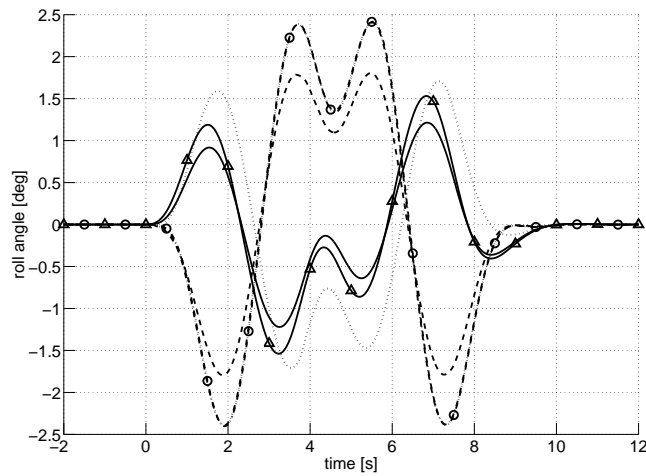
(b) Normalised load transfers. Active roll control: *steer axle* ($\cdots\cdots$), *drive axle* (—), *semi-trailer axles* ($\text{—}\triangle$); passive suspension: *steer axle* (---), *drive axle* ($\cdots\cdots$), *semi-trailer axles* ($\cdots\circ\cdots$).

Figure 10: Response of the linear, torsionally flexible tractor semi-trailer model with a passive suspension or a full-state feedback controller to a step steering input.



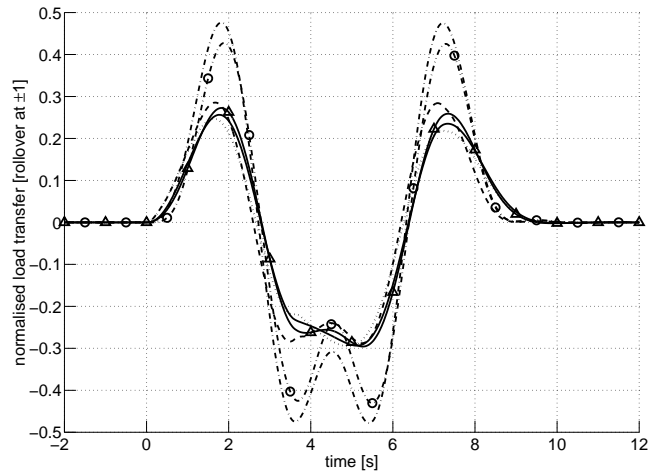
(c) Active anti-roll bar moments. Active roll control: *steer axle* (·····), *drive axle* (—), *semi-trailer axles* (—△—).

Figure 10: Continued.

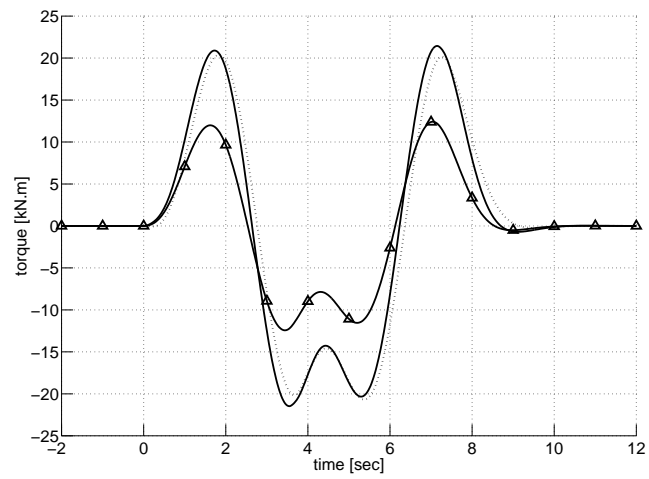


(a) Suspension roll angles. Active roll control: *steer axle* (·····), *drive axle* (—), *semi-trailer axles* (—△—); passive suspension: *steer axle* (---), *drive axle* (·-·-·), *semi-trailer axles* (·-○-·).

Figure 11: Response of the linear, torsionally flexible tractor semi-trailer model with a passive suspension or a full-state feedback controller to a double lane change steering input.

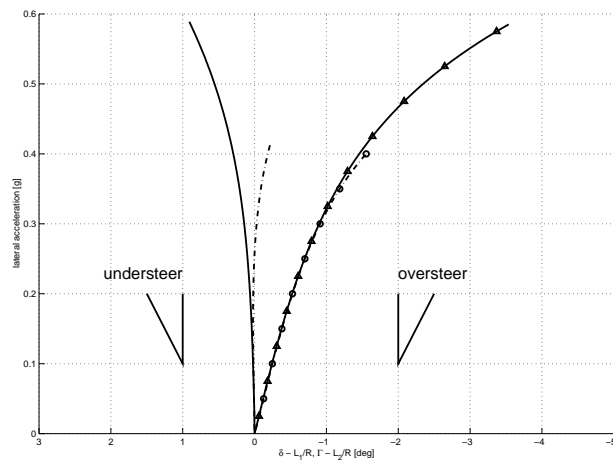


(b) Normalised load transfers. Active roll control: *steer axle* ($\cdots\cdots$), *drive axle* (---), *semi-trailer axles* ($\text{---}\triangle\text{---}$); passive suspension: *steer axle* (---), *drive axle* ($\cdots\cdots$), *semi-trailer axles* ($\cdots\circ\cdots$).



(c) Active anti-roll bar moments. Active roll control: *steer axle* ($\cdots\cdots$), *drive axle* (---), *semi-trailer axles* ($\text{---}\triangle\text{---}$).

Figure 11: Continued.



Active roll control: tractor (—△—), semi-trailer (—△—);
 passive suspension: tractor (· - · - ·), semi-trailer
 (· - o - ·).

Figure 12: Handling diagram of the torsionally flexible tractor semi-trailer with a passive suspension or a full-state feedback controller.